REPORT DOCUMENTATION PAGE

Form Approved
OMB No. 0704-0188

Public reporting burden for this collection of information is estimated to average one hour per response, including the time for reviewing instructions, searching existing data sources, gathering and maintaining the data needed, and completing and reviewing the collection of information. Send comments regarding this burden estimate or any other aspect of this collection of information, including suggestions for reducing the burden to Washington Headquarters Services. Directorate for Informtion Operatins and Reports, 1215 Jefferson Davis Highway, Suite 1204, Arlington, VA 22202-4302. and to the Office of Management and Budget. Paperwork Reduction Project (0704-0188). Washington, DC 20503.

1. AGENCY USE ONLY (Leave blank)	2. REPORT DATE	3. REPORT TYPE AND DATES COVERED
	6/19/97	Final Technical Report 12/1/j94 - 11/30/96

4. TITLE AND SUBTITLE
Archive and Analysis of Oceanographic and Meteorological Data

5. FUNDING NUMBERS
G N00014-95-1-0146

6. AUTHOR(S)
Nancy A. Bray, Principal Investigator

7. PERFORMING ORGANIZATION NAMES(S) AND ADDRESS(ES)
Center for Coastal Studies
Scripps Institution of Oceanography
La Jolla, CA 92093-0209

8. PERFORMING ORGANIZATION REPORT NUMBER

9. SPONSORING/MONITORING AGENCY NAME(S) AND ADDRESS(ES)
Steven R. Ramp
Office of Naval Research
Physical Oceanography, Code 322PO
800 North Quincy Street
Arlington, VA 22217-5500

10. SPONSORING/MONITORING AGENCY REPORT NUMBER

19970623 293

11. SUPPLEMENTARY NOTES

12a. DISTRIBUTION/AVAILABILITY STATEMENT
Unrestricted

DISTRIBUTION STATEMENT A
Approved for public release
Distribution Unlimited

12b. DISTRIBUTION CODE

13. ABSTRACT (Maximum 200 words)

The objectives of the grant were to locate, convert and archive historical data from the Red Sea, and to make those data available on-line to researchers interested in that region, and secondly, to begin comparison of those historical data with NAVOCEANO's real-time circulation model of the Red Sea.

The data are archived in a standard, flat ASCII, self-documenting form and can be found at the internet web site:

gopher://gopher-ccs.ucsd.edu:70/11/zoo/redsea.

This can also be reached via the Scripps Center for Coastal Studies Home Page: http://www-ccs.ucsd.edu, and accessing the Data Zoo, and then redsea on that page. A print-out of the Red Sea data archive main directory page is attached as Appendix A to this report.

Comparisons between the NAVOCEANO Red Sea model output and observations from the archive are describe in a report previously submitted to the program managers for this project, and is also attached as Appendix B to this report.

14. SUBJECT TERMS
Red Sea, real-time circulation

15. NUMBER OF PAGES
23

16. PRICE CODE

17. SECURITY CLASSIFICATION OF REPORT	18. SECURITY CLASSIFICATION OF THIS PAGE	19. SECURITY CLASSIFICATION OF ABSTRACT	20. LIMITATION OF ABSTRACT
Unrestricted	Unrestricted	Unrestricted	None

APPENDIX A
Data archive main directory

BRAY
FINAL REPORT
N00014-95-1-0146

Gopher Menu

AODC

Gidon

Maillard

NODC

Quadfasel

figures.html [27May97, 2kbl

images

redsea.html [9Jun97, 3kbl

redsea.html.old [12Nov96, 4kbl

report

text

gopher://gopher-ccs.ucsd.edu:70/11/Zoo/redsea.

APPENDIX B

BRAY
FINAL REPORT
N 00014-95-1-0146.

DRAFT REPORT
September, 1996

Semi-permanent gyres in the Red Sea: a comparison of numerical model and observational results

Nan Bray, Thomas Moore
Scripps Institution of Oceanography

Melody Clifford, Charles Horton
NAVOCEANO

Abstract

A semi-permanent gyre in the northern Red Sea, identified from observations by Quadfasel and Baudner [1993; hereafter QB], also appears in the NAVOCEANO sigma-coordinate model of the Red Sea. The model is forced by real-time atmospheric fields as estimated by NORAPS and NOGAPS products. Over the model period of mid-1993 to late 1994, the gyre was found to be remarkably persistent in structure and transport, and similar to the observed gyres, measured in the period 1983 to 1987. Transport associated with the gyre in the top 100m is about 2 Sv, in good agreement with the estimates of QB. Over the top 300m, the depth extent of the gyre, the recirculating transport is 4 Sv. Circulation in the gyre is strongest in summer, and weakest in winter. The model gyre appears to migrate northward of 23 N in fall and winter, by about its radius distance. The observational gyre may have the same behavior, but if so, it is not well-resolved by the transects available. The migration suggests that the gyre responds to time-dependent atmospheric forcing as well as to the local bathymetry.

1. Introduction

This is a preliminary report on work in progress, in which the detailed circulation patterns of the Red Sea are examined both from observations and from the real-time NAVOCEANO sigma-coordinate model of the Red Sea. The work is focused on identifying the relative contributions to the observed variance of wind and thermohaline forcing. In this report, we compare the model and observational evidence for a semi-permanent gyre in the northern Red Sea, near 23 N. Because the Red Sea is narrow (200km wide by 2000 km long) and has strong thermohaline forcing much of the focus of past research has been on the resultant vertical circulation of relatively fresh surface waters flowing into the sea from the Gulf of Aden, and relatively saline water, transformed by extensive evaporation, flowing out of the sea at depth. In comparison, little attention has been given to the equally strong wind-driven component of circulation in the Red Sea. As early as 1962, Neumann and McGill discussed observational evidence for three-dimensional flow in the Red Sea, and Maillard [1971] described a number of basin-width gyres in hydrographic and GEK surveys. Quadfasel and Baudner [1993] used a recent series of hydrographic and XBT surveys to identify gyres that are semi-permanent at severa locations in the Red Sea. The most persistent of these is an anticyclonic gyre located near 23 N, and was observed in all four seasons and all but three of the 25 along-axis sections QB analyzed. We looked for the same feature in the model results.

2. Analysis of the model gyre

The NAVOCEANO model is run in real-time, and is used as an operational forecasting model. To do the analysis described below, we used the "restart" files generated by the model every 2 or 4 weeks, over the period mid-1993 to late 1994. A total of 23 files were used (Table 1), and we grouped them into the four seasons, with winter defined as December, January and February, and the other seasons following in sequence. There are between 4 and 8 realizations of model results in each season. Variables that are included in the restart files are: along- and across-sea velocities (v and u), potential temperature, salinity and potential density. The grid of the model is set up to run approximately along and across the sea; v and u are the grid velocities--we have not done any additional rotation to align them with principal axes or more closely with the bathymetry. The restart files are loaded into a Silicon Graphics program called Explorer, which we use to make the vertical and horizontal cuts for each file. The cuts are then analyzed using Matlab. For the following analysis, we examine the east-west grid line centered at 23 N. We have not averaged the data in the along-axis direction.

3. The gyre at 23 N

The model gyre is most readily seen in the along-axis velocity v (Figure 1). It is present in all four seasons, and the core extends to a depth of 200 m. Maximum speeds are 0.5 m/s, and the strongest recirculation occurs in summer. The transport per unit width, integrated over the top 100 m (Figure 2) and top 300 m (Figure 3) illustrates the anticylonic circulation pattern quite clearly. Note that in winter and to a lesser extent in fall there is a larger cross-axis component of velocity (u), also shown in the cross-section plots of u (Figure 4). We have interpreted this as a migration of the gyre northwards in those seasons. Also shown in Figures 2 and 3 is the average standard deviation in transport (per unit width) over the section, to the depth of integration (100 or 300m). It appears as an arrow at the origin of each subplot. The seasonal mean transports in the gyres are significantly larger than the standard deviations. The recirculating and residual transports (based on v), integrated across the section are given in Table 2. To determine the recirculating transport, we integrated the northward and southward velocities separately, and then took the average of the absolute values of those transports. The residual is calculated as the difference between the (absolute) northward and southward transports. The recirculating transports are comparable to those estimated by QB for the top 100 m, who found a range of about 0.4 to 2.8 Sv. The model gyres have seasonal average transports of 1.0 to 2.7 Sv. Transports over the top 300 m are nearly twice the 100m transports, not surprising in view of the fact that the gyre extends to more than 200 m depth.

Density and temperature structure in the model gyre is similar to the observed gyres (Figures 5 and 6; compare with QB figures 2a and 2c). However, the model salinity does not reproduce the observed field particularly well. In Figure 7, the salinity anomaly (S-40)*100 is plotted. The range in salinity is smaller than that observed (see e.g. QB figure 2b), and the model salinity is overall too high by about 0.5 psu. Fortuitously, this doesn't affect the gyre circulation very much, since the observed T/S relationship is quite linear, and temperature and salinity are

reasonably well-correlated. QB used that fact to estimate gyre transports from XBT temperature sections alone.

For each of the mean fields from the model we also calculated standard deviations over the corresponding period, and those are illustrated in the Appendix, along with black and white versions of the mean field contour plots. In general, the spatial variations of the mean fields are statistically significant, in both the seasonal and the overall averages.

4. Summary and future work

The model appears to reproduce the semi-permanent gyre at 23 N remarkably well. The model results further suggest that the gyre may migrate by 100 km or so to the north in fall and winter, a result that is not obvious from the observational analysis. In the continuing work on this project, we expect to re-examine the QB data to see if there is any clear observational evidence for seasonal migration of the gyre, and also to look for possible forcing mechanisms for the migration in the model winds.

Another analysis we have begun, but not yet completed, is to look at along-axis sections in the same way that we did the 23N cross-section, to see if we can identify the gyres found farther south in the Red Sea by QB. Those gyres are less persistent, and occasionally cyclonic, so that will be a somewhat more stringent test of the model.

We also plan to examine the salinity structure in the model in comparison to the observations more generally, and see if we can make some recommendations on how to improve the model's simulation of the salinity field.

References

Maillard, C., 1971: Etude hydrologique et dynamique de la Mer Rouge en hiver, Annls Inst. Oceanogr. Paris, 498(2), 113-140.

Neumann, A. C. and D. A. McGill, 1962: Circulation of the Red Sea in summer, Deep-Sea Res. 8, 223-235.

Quadfasel, D. and H. Baudner, 1993: Gyre-scale circulation cells in the Red Sea, Oceanologica Acta 16(3), 221-229.

List of Figures

Figure 1: Along-axis velocity (v) through a cross-section centered at 23 N.

Figure 2: Vector transport per unit width, integrated from 100 m to the surface. The average standard deviation in the transport is shown by the arrow at the origin of each subplot. Up is northward along the axis of the Red Sea.

Figure 3: As for Figure 2, except integrated over the top 300 m.

Figure 4: Across-axis velocity (u) through a model cross-section centered

at 23 N.

Figure 5: Potential density of a model cross-section centered at 23 N.

Figure 6: Potential temperature of a model cross-section centered at 23 N.

Figure 7: Salinity anomaly (S-40)*100 of a model cross-section centered at 23 N.

Appendix figures:

Mean and standard deviations of: potential temperature, potential density, salinity anomaly (S-40)*100, cross-axis and along-axis velocities (u and v). Statistics are calculated over each season, and over all the restart files (see Table 1 for the number of realizations in each season).

Table 1: Inventory of restart files used in the analysis (Julian day and year)

Winter: 34093, 36093, 02094, 04094

Spring: 06094, 08094, 10094, 12094, 14094

Summer: 18093, 20093, 22093, 24093, 16094, 18094, 20094, 22094

Fall: 26093, 28093, 30093, 32093, 26094, 30094

Table 2: Transports (Sv) associated with the gyre at 23 N

Season	Top 100 m		Top 300 m	
	Recirculating transport	Residual transport	Recirculating transport	Residual transport
Winter	2.3	-0.3	4.0	-0.9
Spring	2.7	-0.4	4.6	-0.3
Summer	3.3	-0.2	5.7	-0.8
Fall	1.0	-0.3	3.9	-0.8
Overall	2.4	-0.02	4.4	-0.7

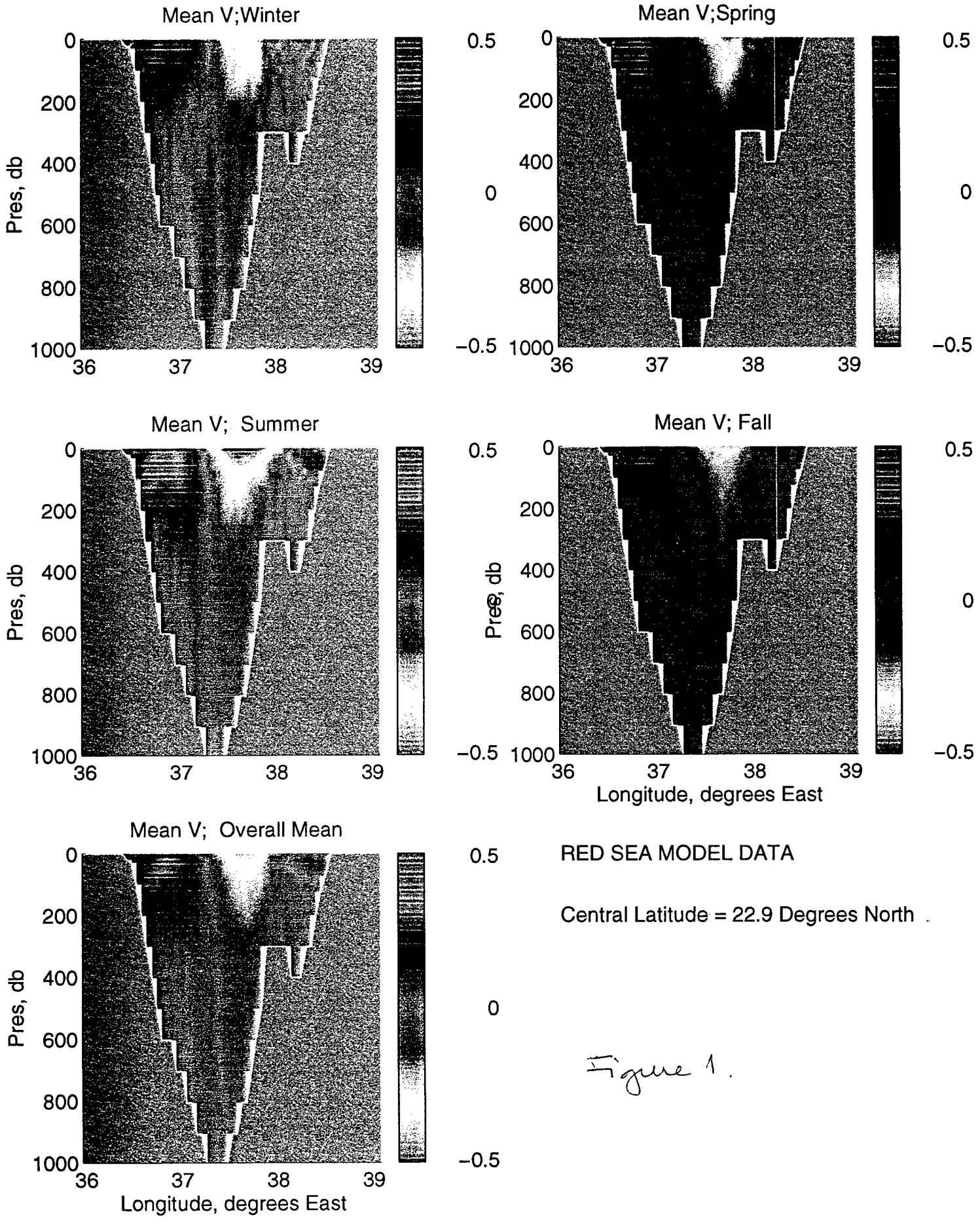
Mean V;Winter
Mean V;Spring
Mean V; Summer
Mean V; Fall
Mean V; Overall Mean
Pres, db
0
200
400
600
800
1000
36
37
38
39
0.5
0
−0.5
Longitude, degrees East
RED SEA MODEL DATA
Central Latitude = 22.9 Degrees North

Figure 1.

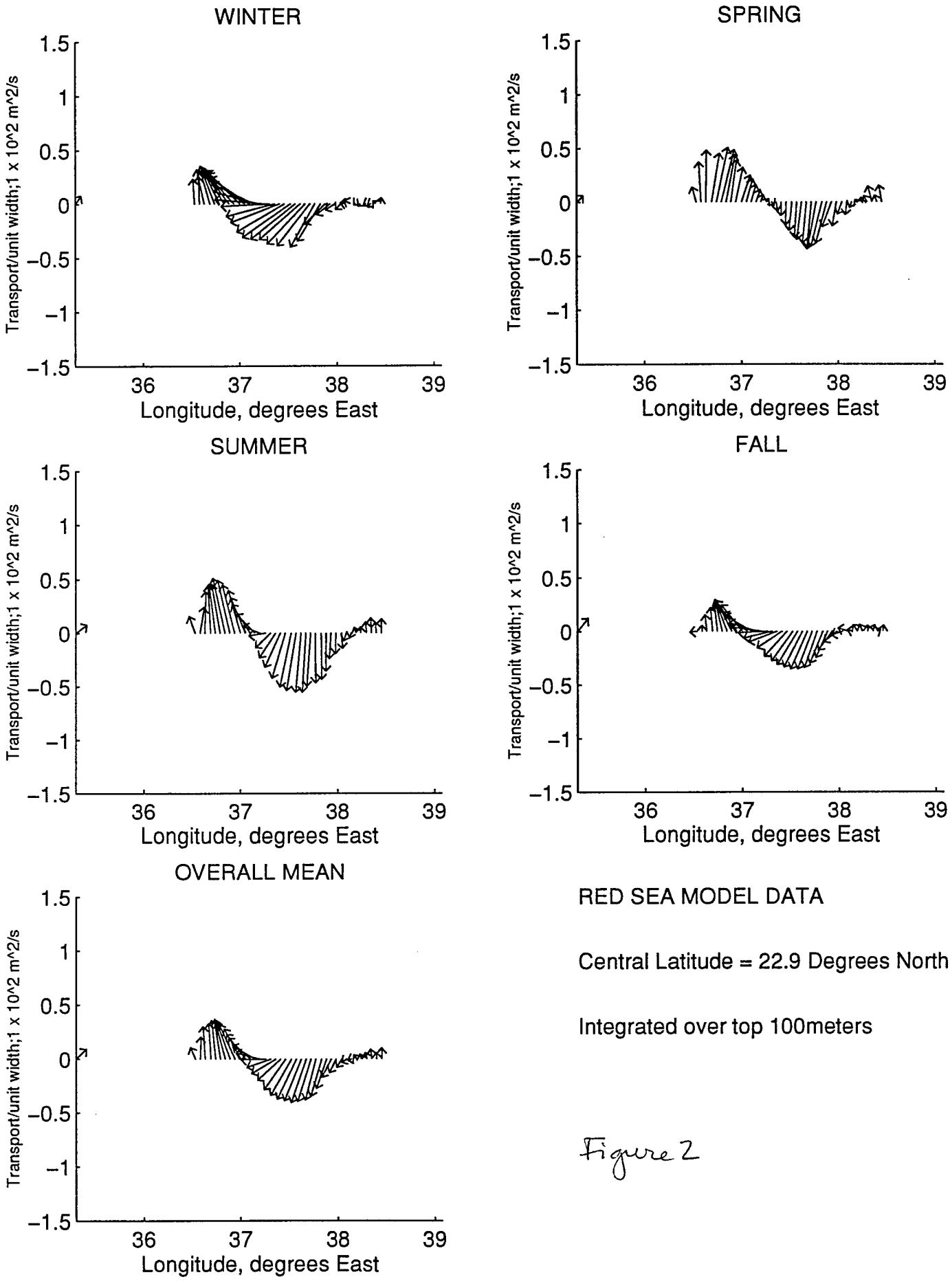

RED SEA MODEL DATA

Central Latitude = 22.9 Degrees North

Integrated over top 100meters

Figure 2

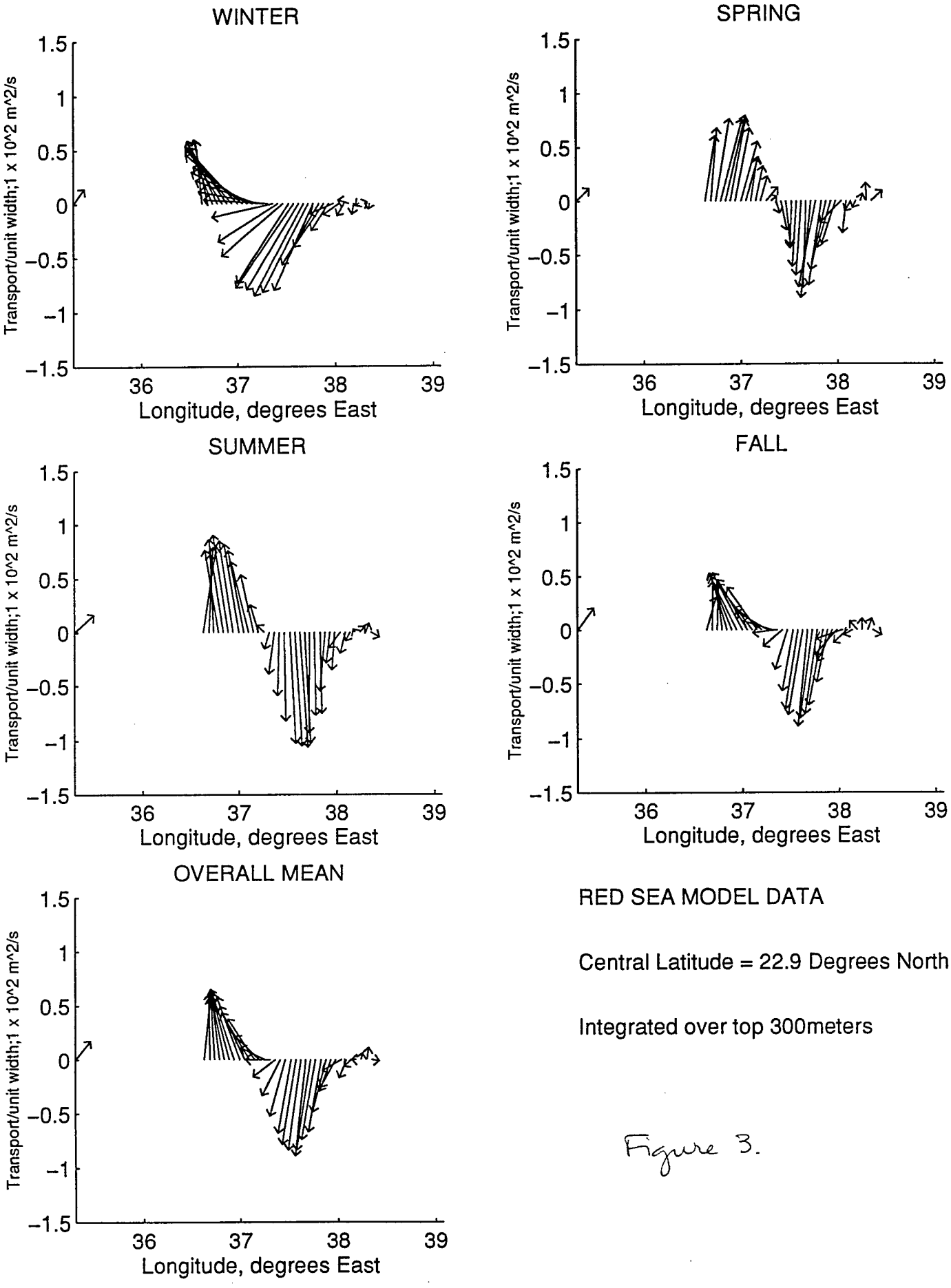

RED SEA MODEL DATA

Central Latitude = 22.9 Degrees North

Integrated over top 300meters

Figure 3.

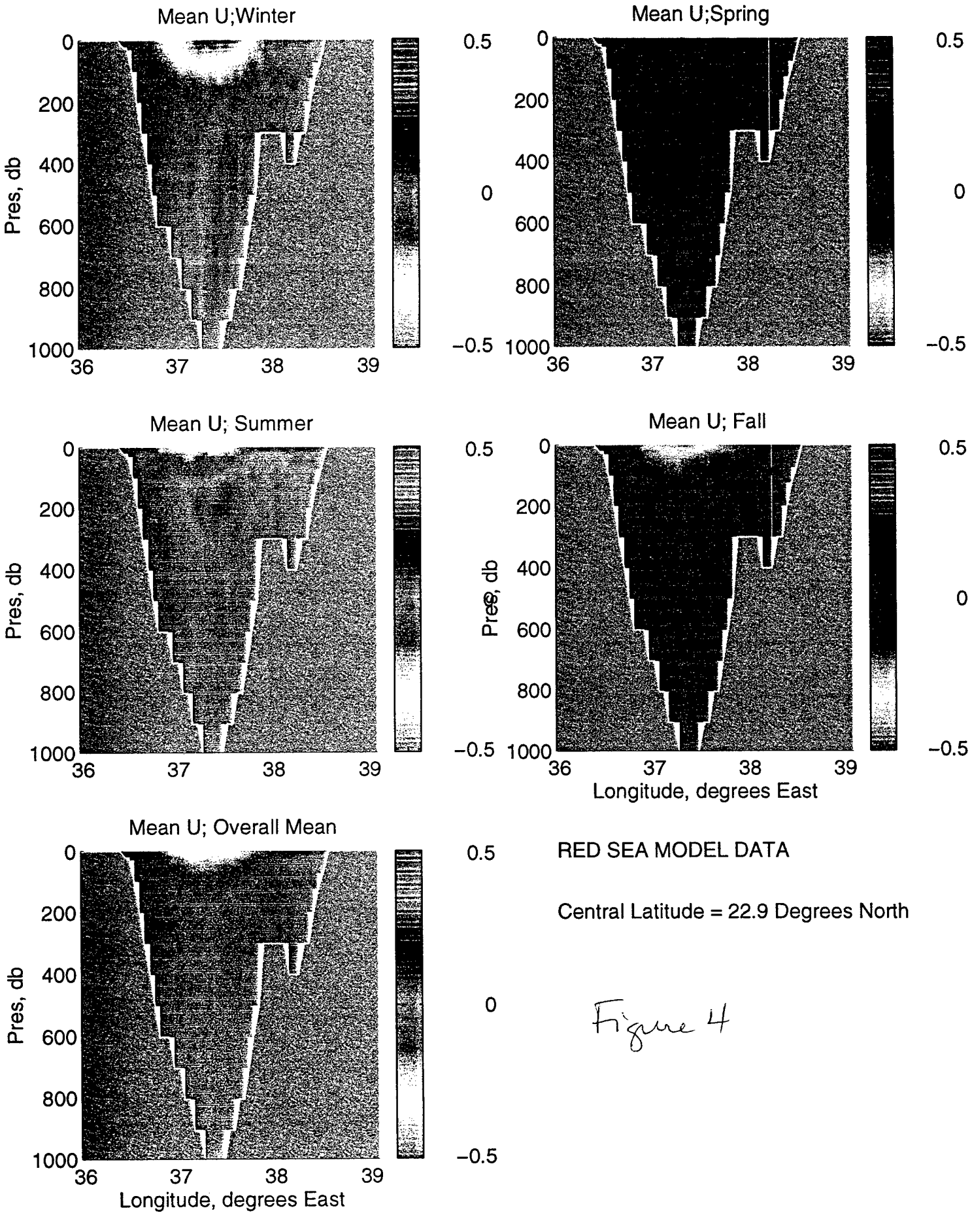
Mean U;Winter
Mean U;Spring
Mean U; Summer
Mean U; Fall
Mean U; Overall Mean
Pres, db
0
200
400
600
800
1000
36
37
38
39
0.5
0
−0.5
Longitude, degrees East
RED SEA MODEL DATA
Central Latitude = 22.9 Degrees North

Figure 4

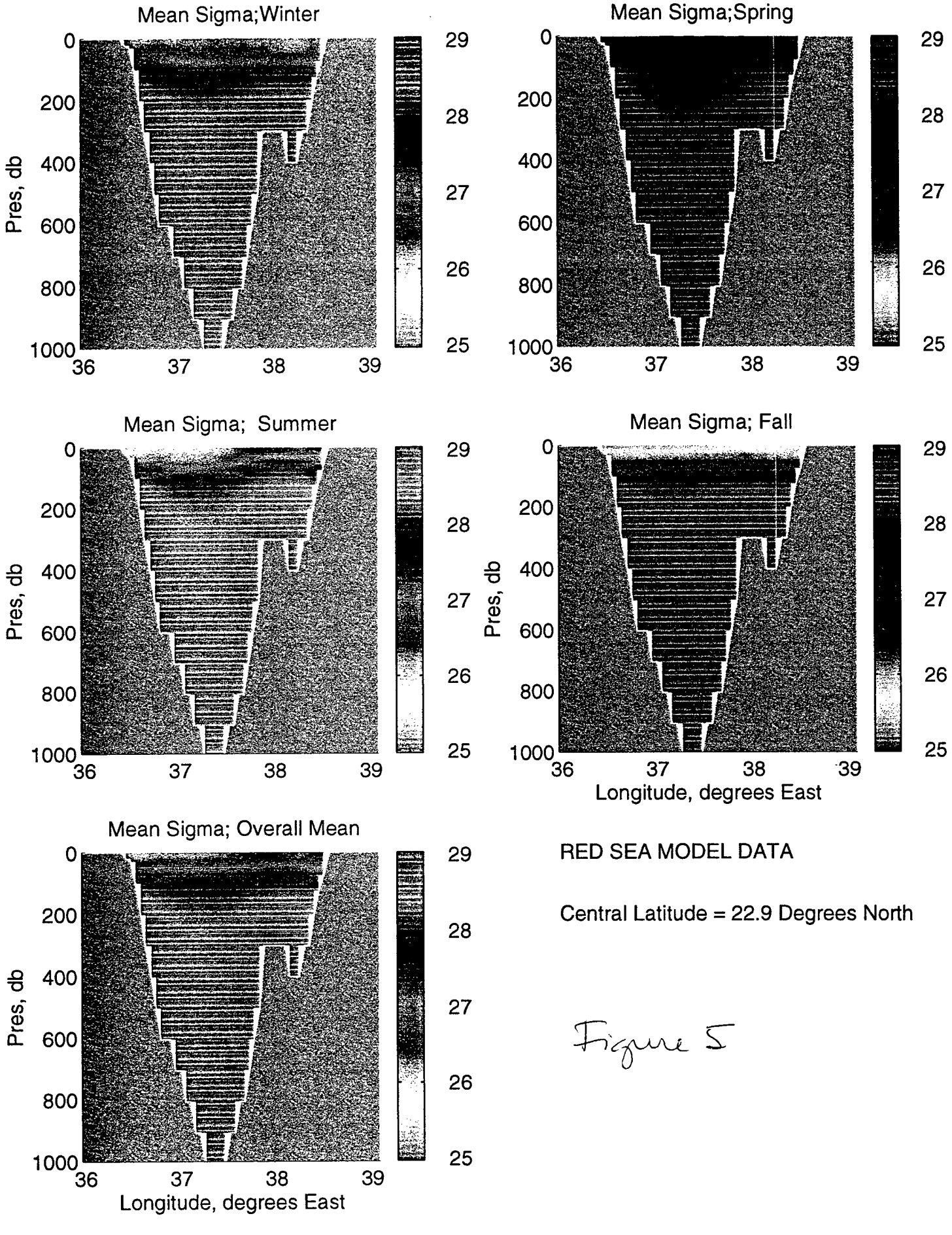

RED SEA MODEL DATA

Central Latitude = 22.9 Degrees North

Figure 5

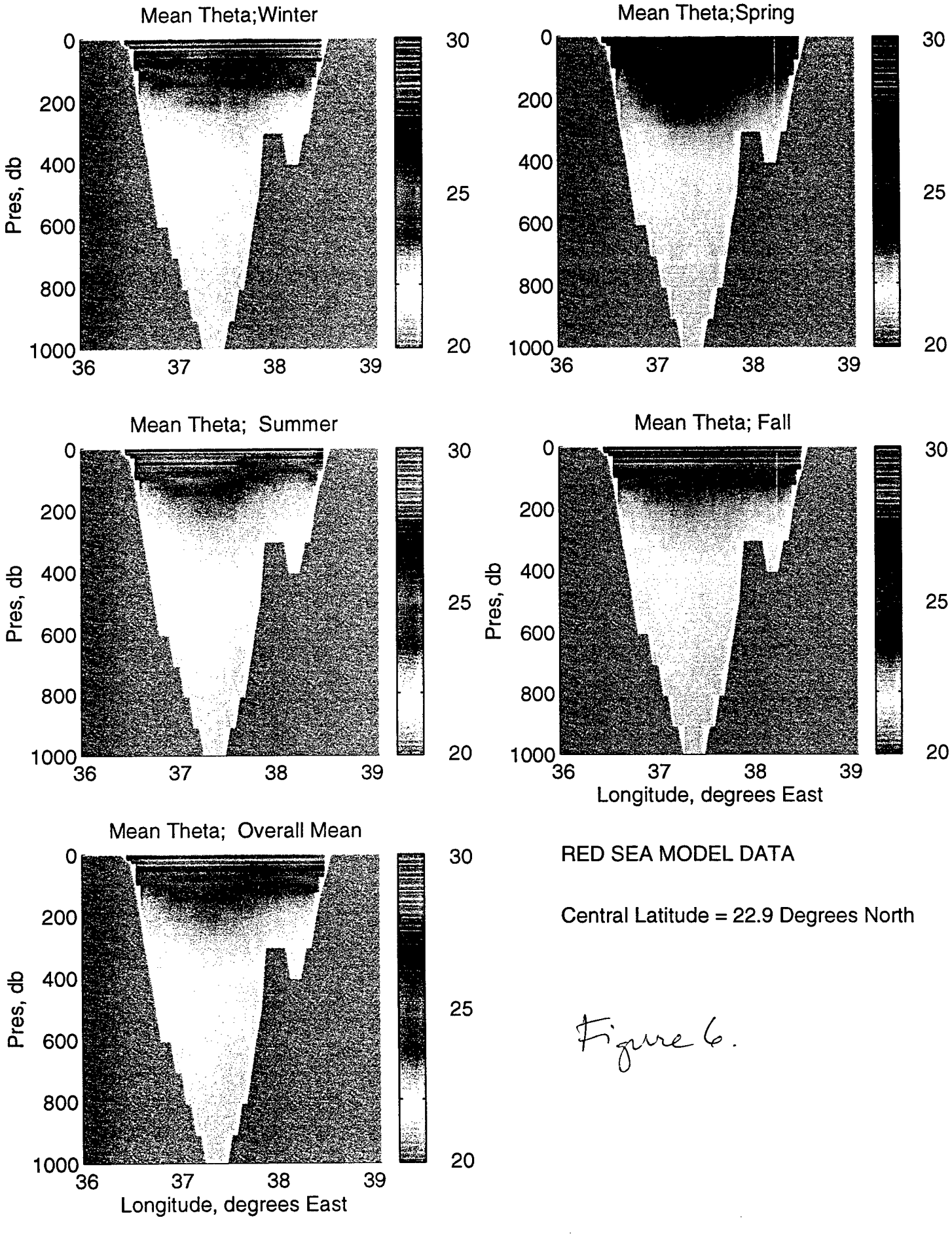
Mean Theta;Winter
Mean Theta;Spring
Mean Theta; Summer
Mean Theta; Fall
Mean Theta; Overall Mean
Pres, db
0
200
400
600
800
1000
36
37
38
39
30
25
20
Longitude, degrees East
RED SEA MODEL DATA
Central Latitude = 22.9 Degrees North

Figure 6.

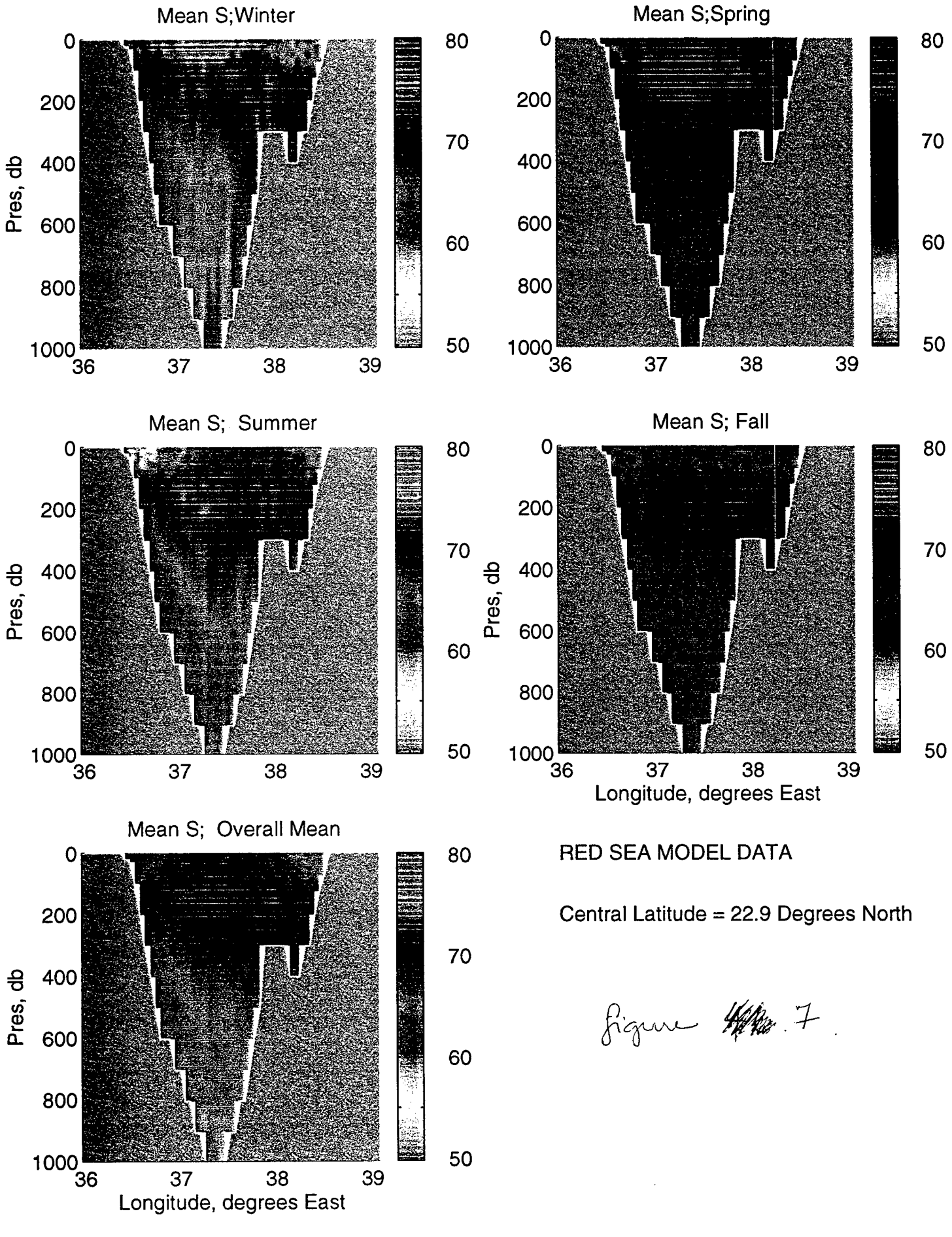
Mean S;Winter
Mean S;Spring
Mean S; Summer
Mean S; Fall
Mean S; Overall Mean
Pres, db
0
200
400
600
800
1000
36
37
38
39
80
70
60
50
Longitude, degrees East
RED SEA MODEL DATA
Central Latitude = 22.9 Degrees North
Figure 7.

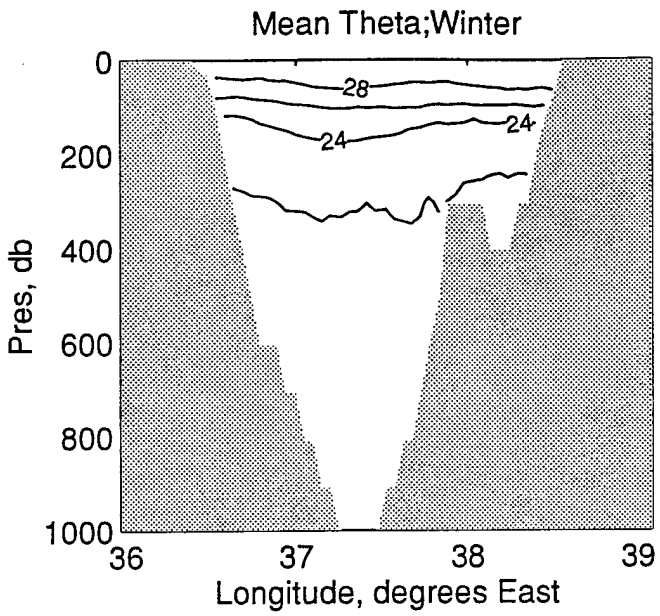

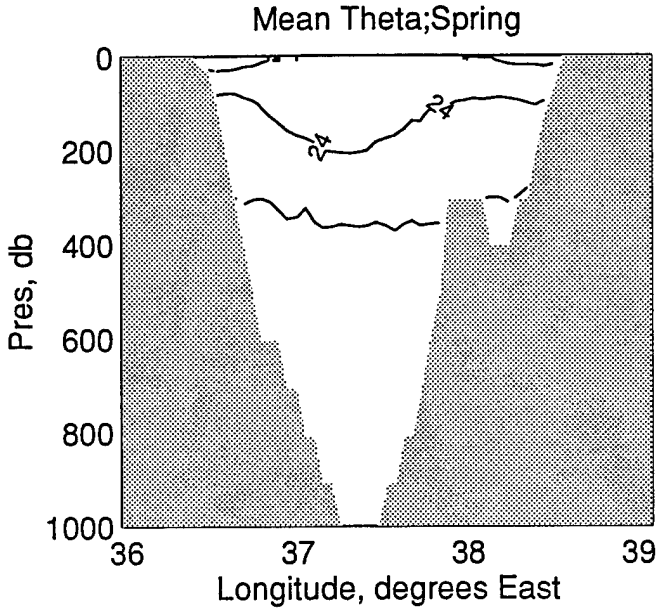

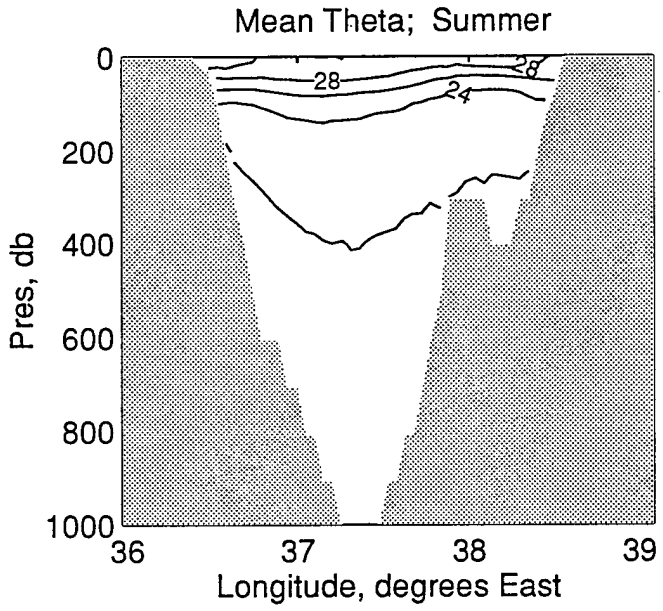

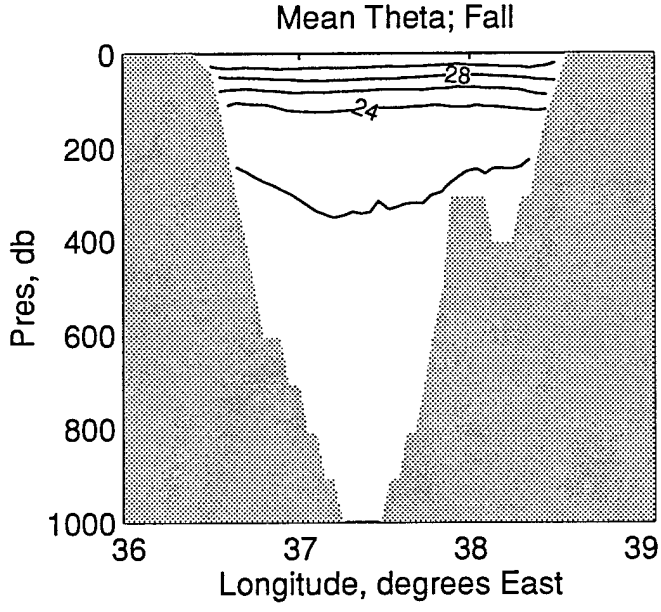

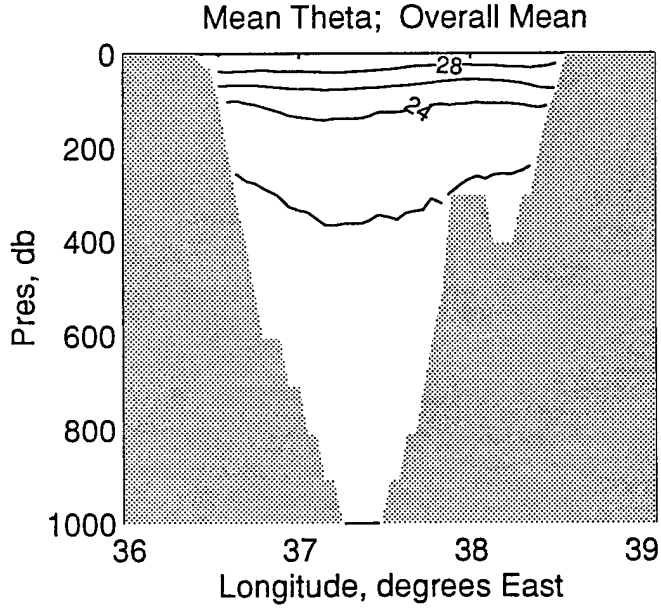

RED SEA MODEL DATA

Central Lattitude = 22.9 Degrees North

Figure A1

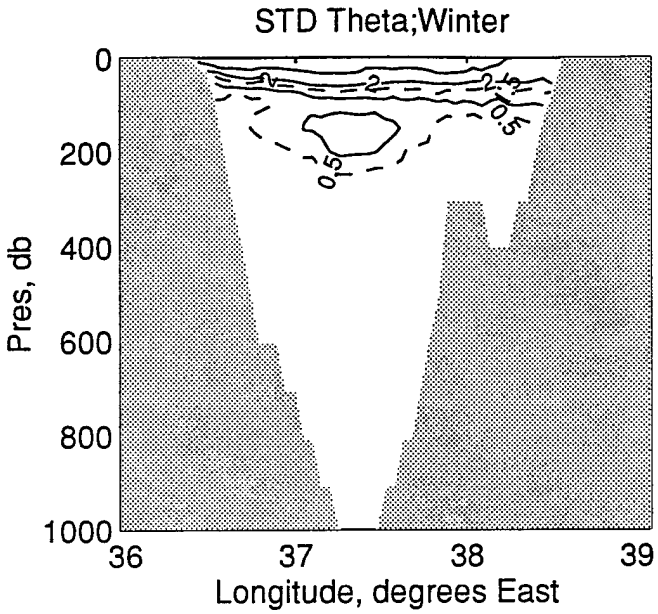

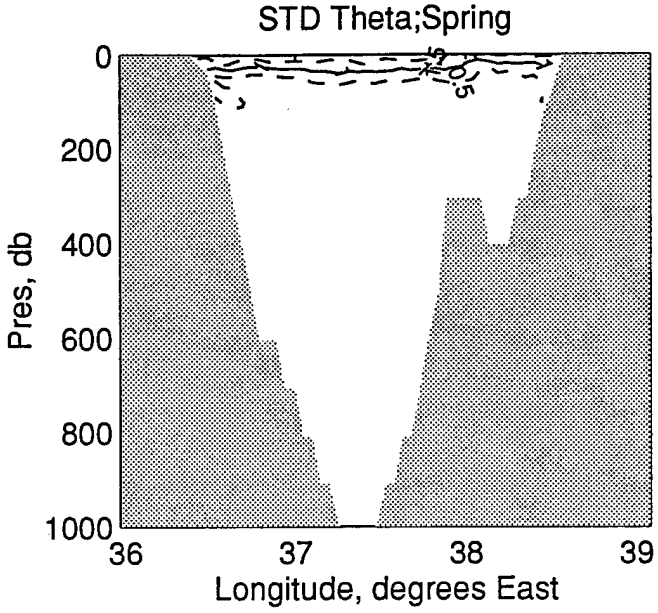

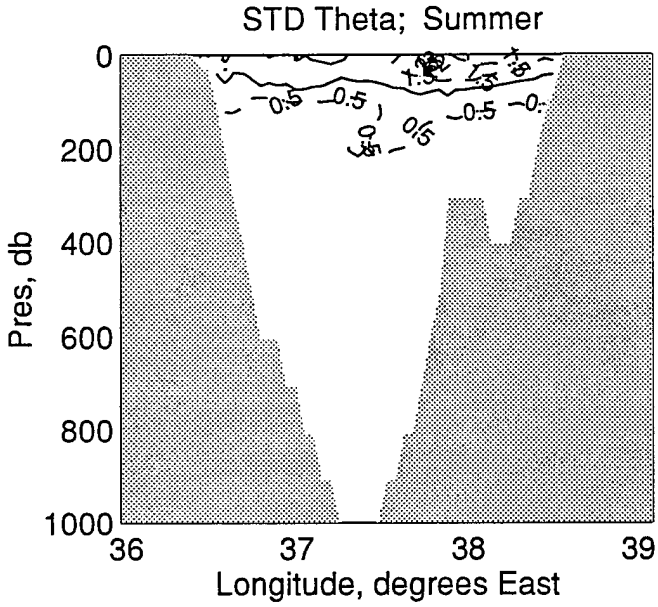

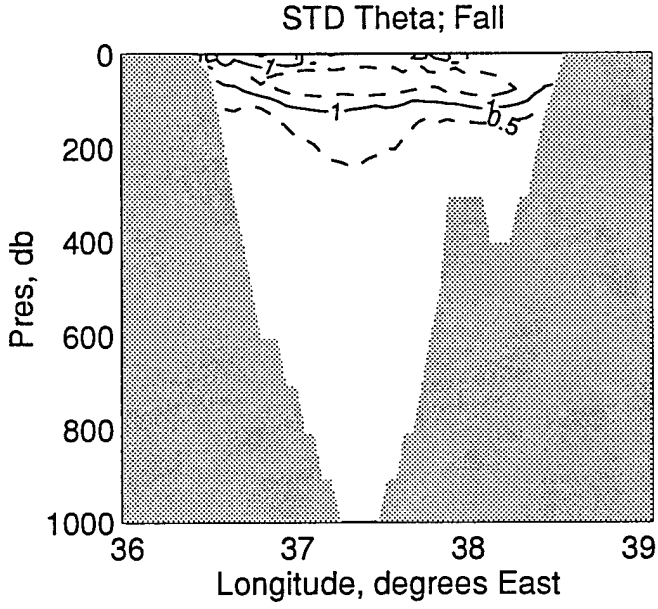

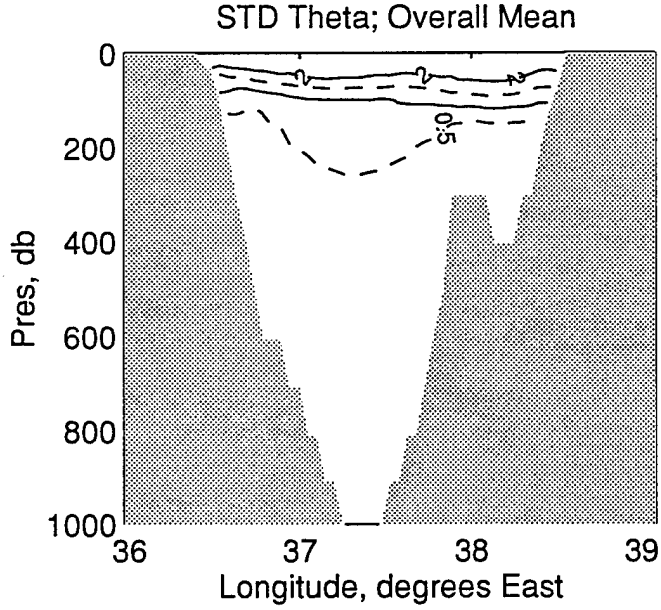

RED SEA MODEL DATA

Central Lattitude = 22.9 Degrees North

Figure A2

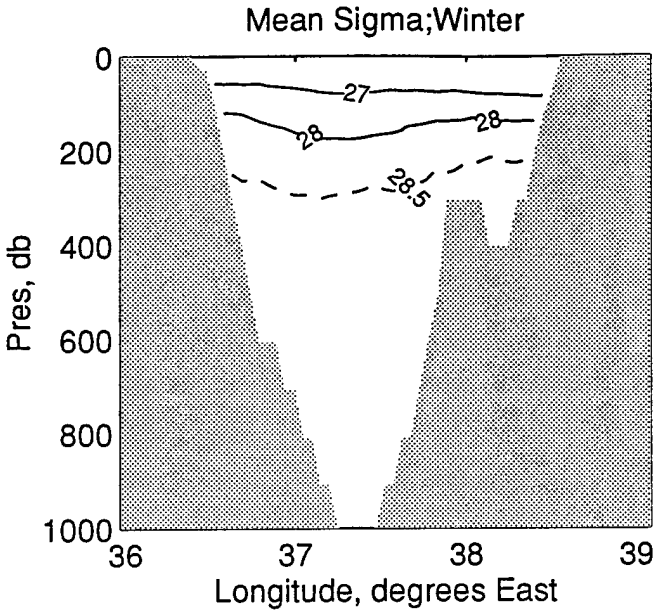

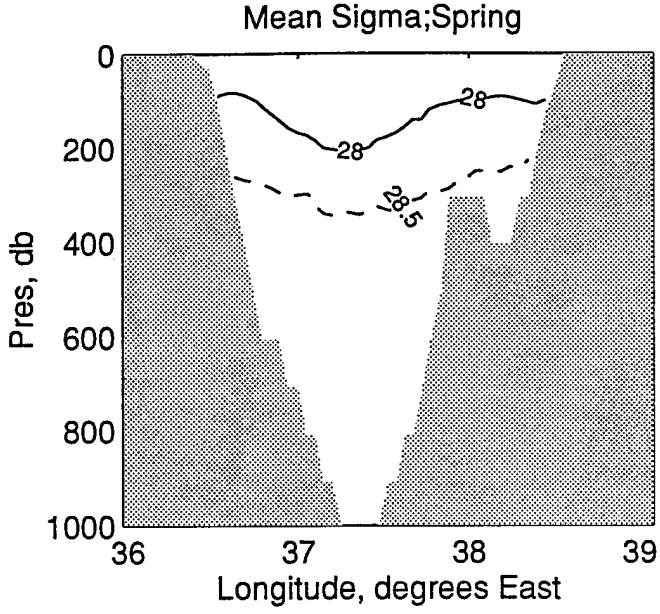

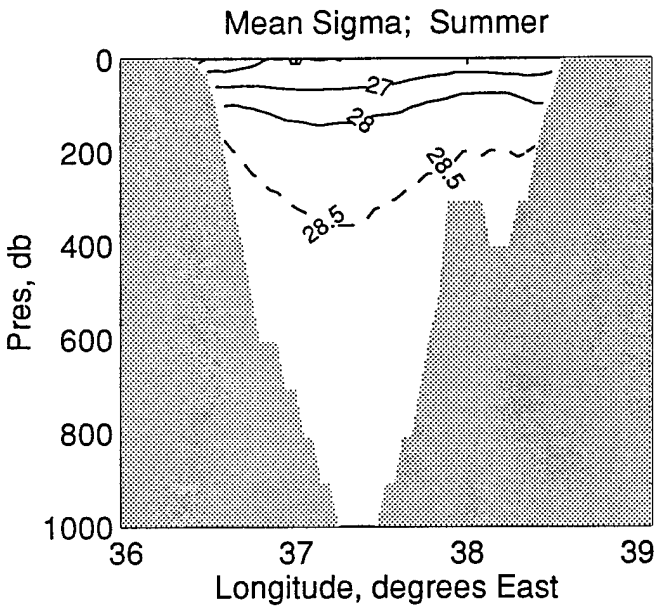

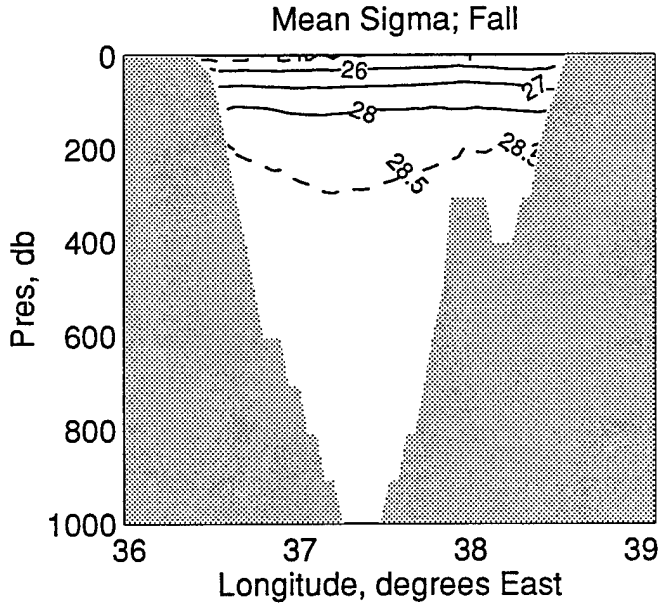

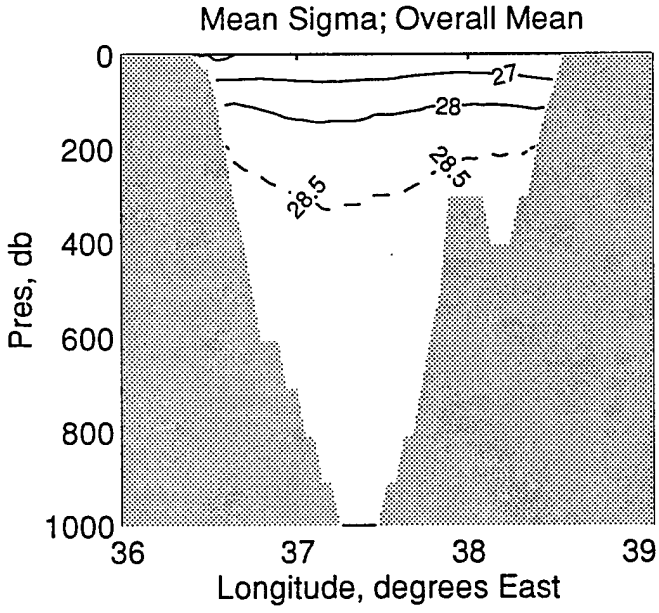

RED SEA MODEL DATA

Central Lattitude = 22.9 Degrees North

Figure A3

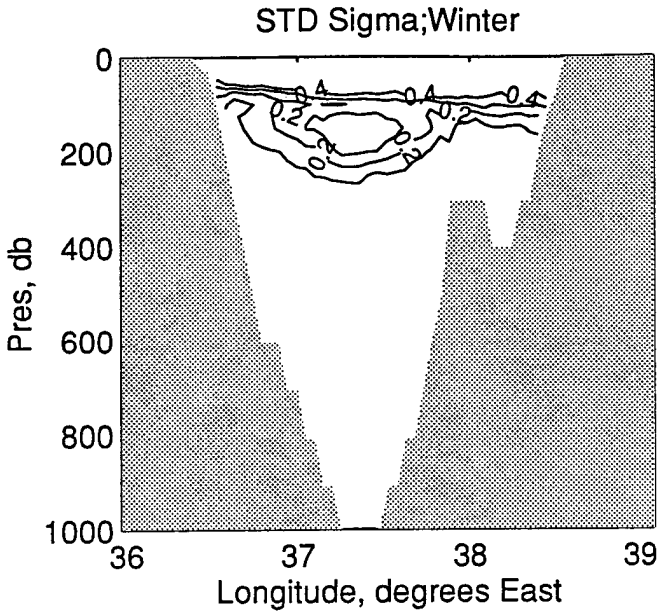

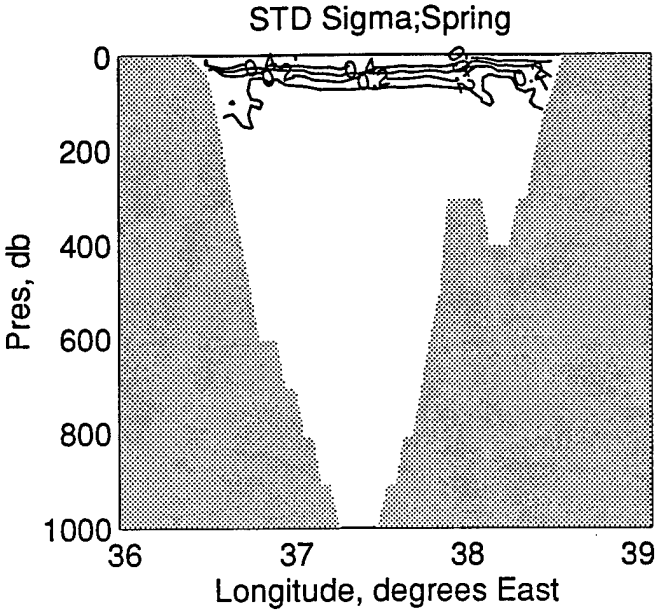

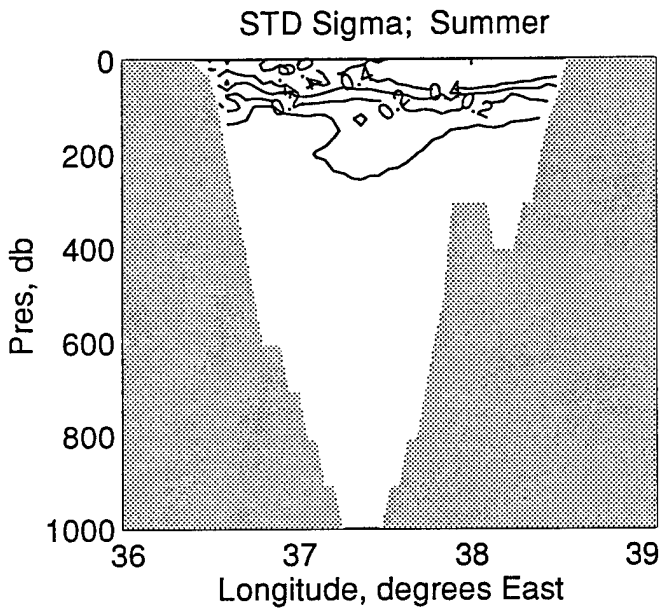

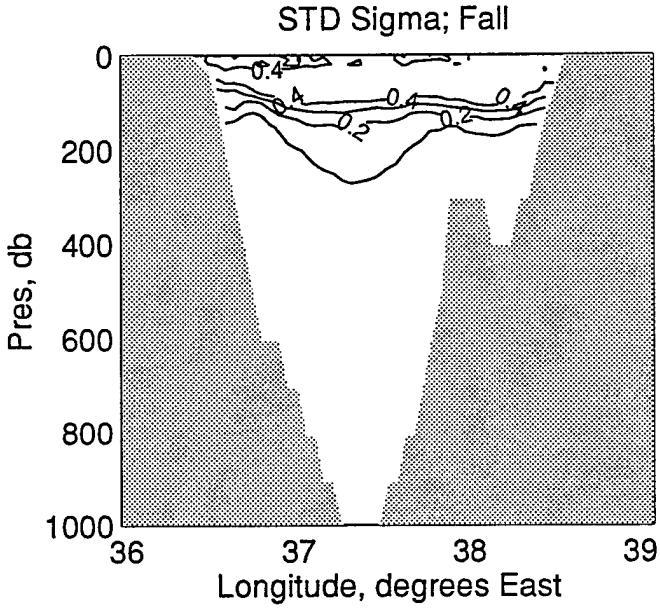

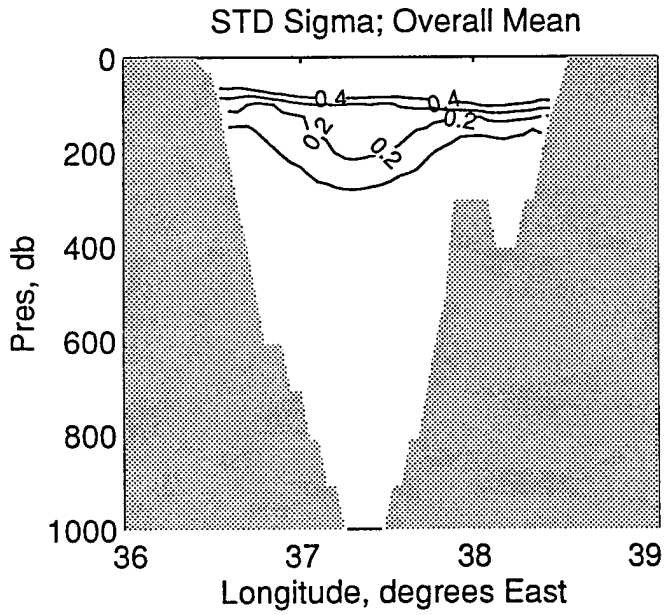

RED SEA MODEL DATA

Central Lattitude = 22.9 Degrees North

Figure A4

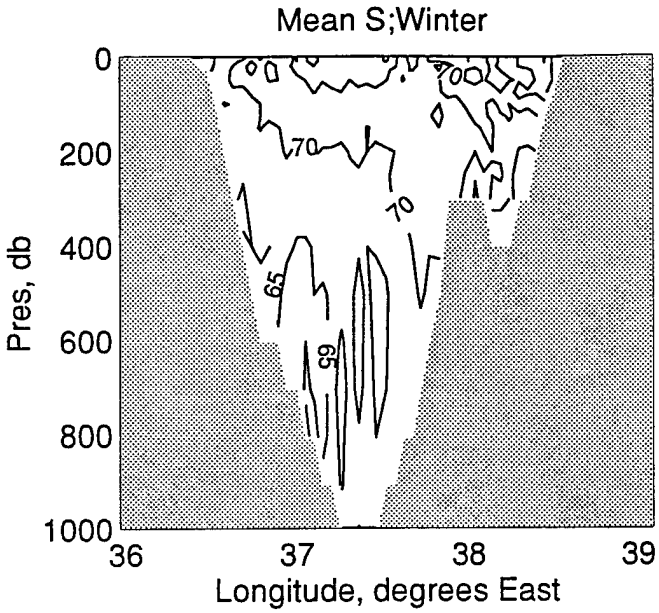

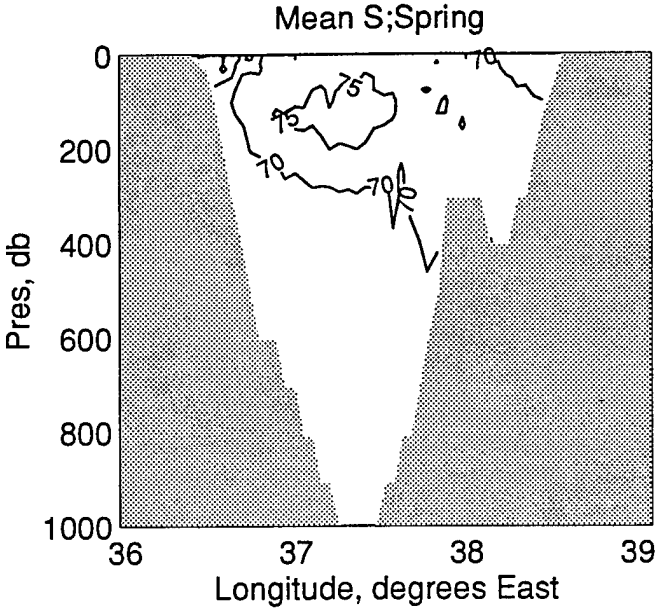

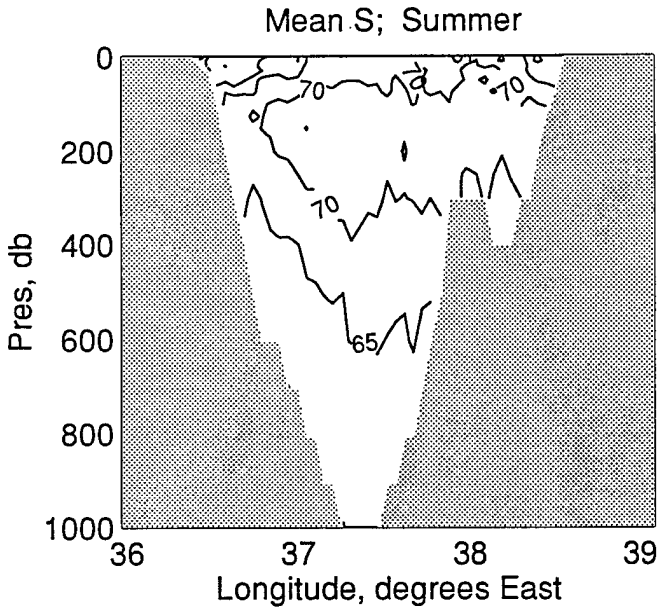

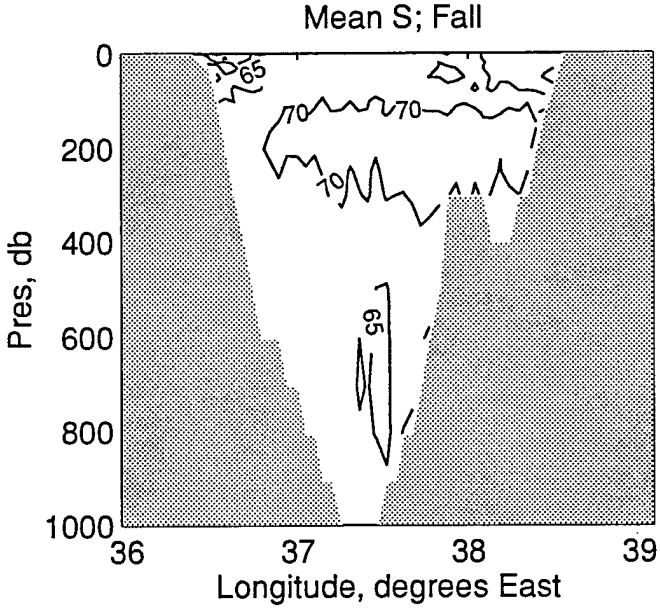

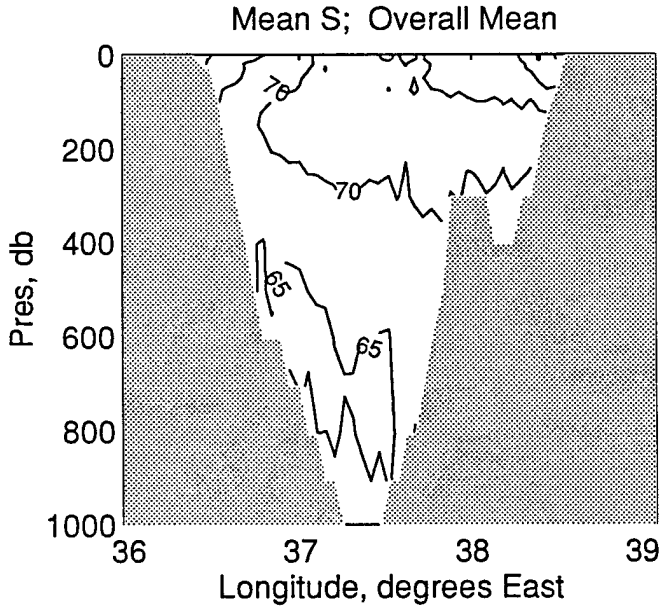

RED SEA MODEL DATA

Central Lattitude = 22.9 Degrees North

Figure A5

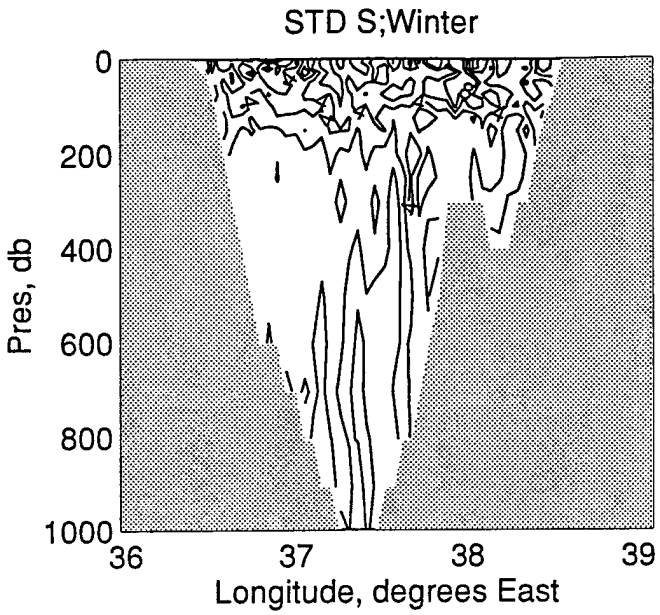

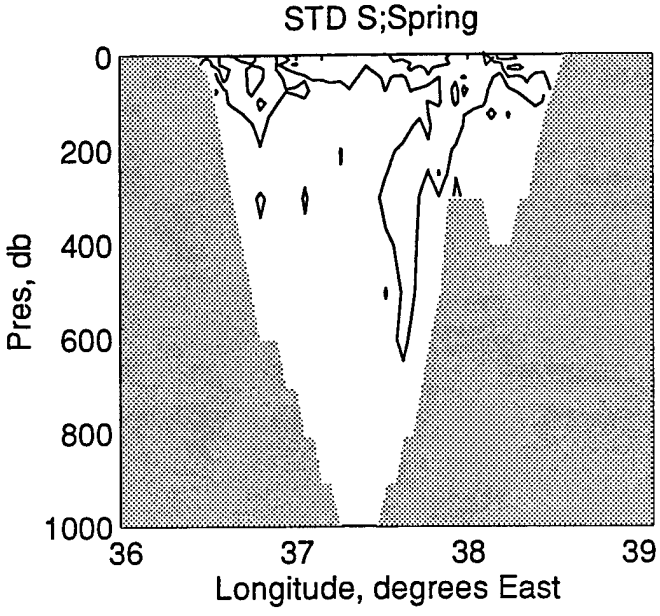

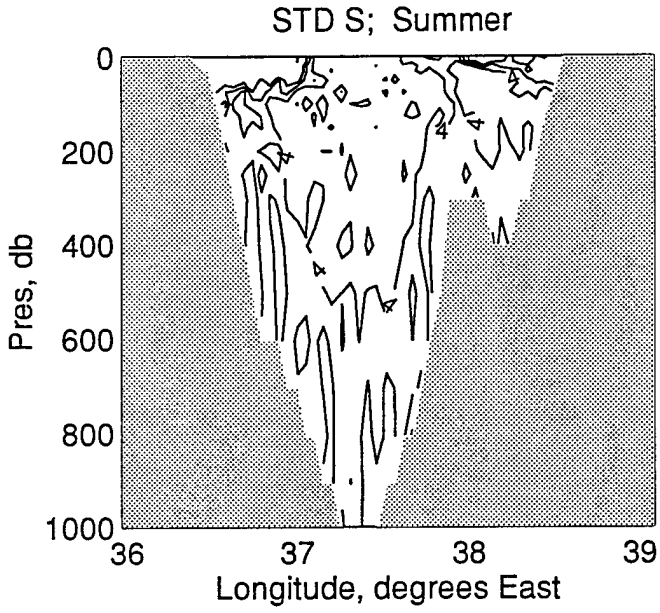

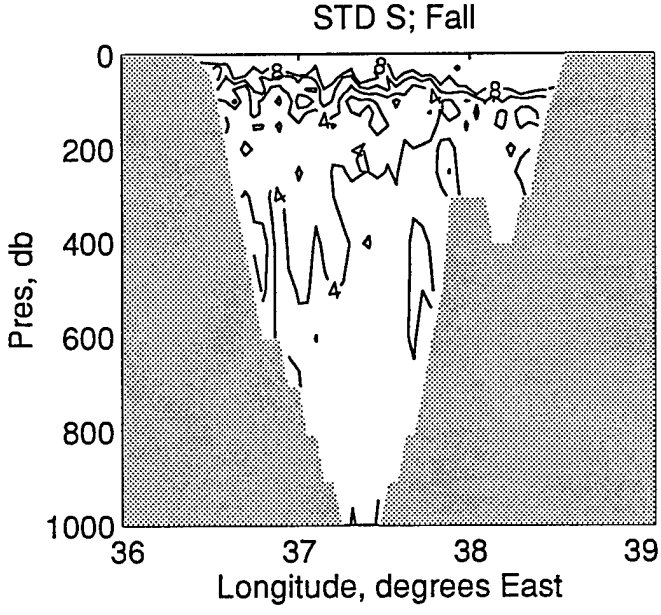

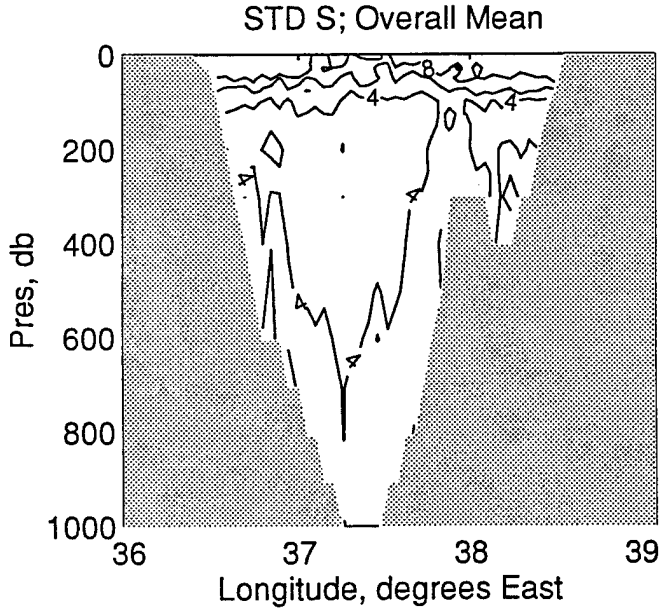

RED SEA MODEL DATA

Central Lattitude = 22.9 Degrees North

Figure A6

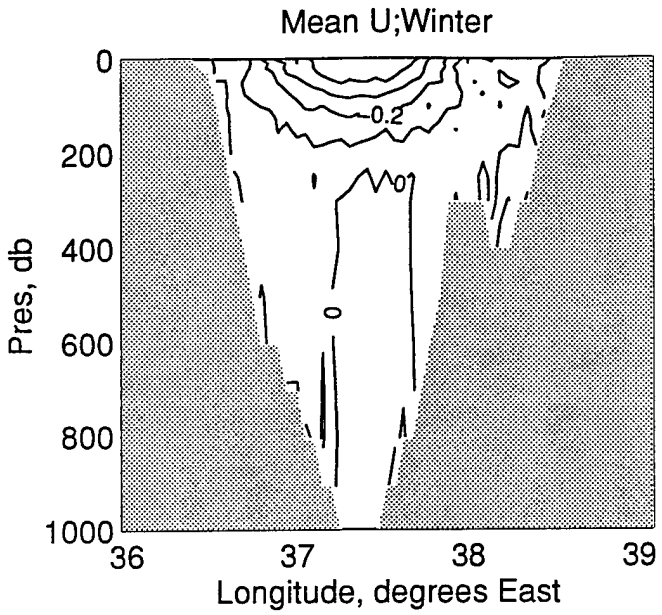

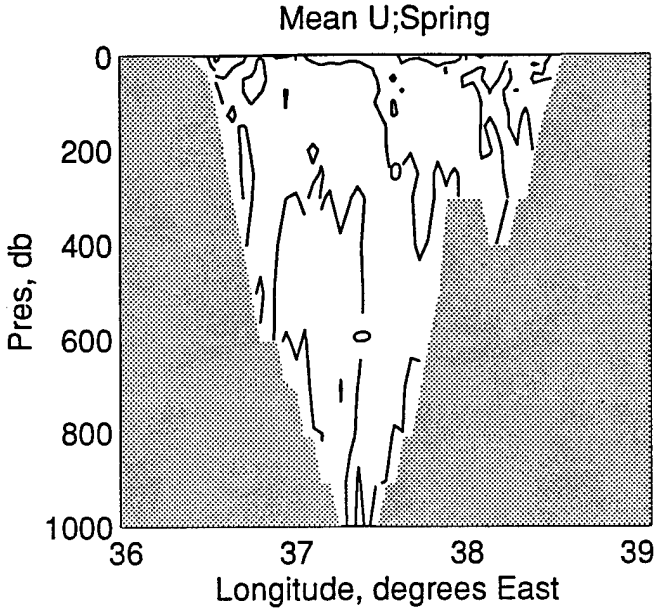

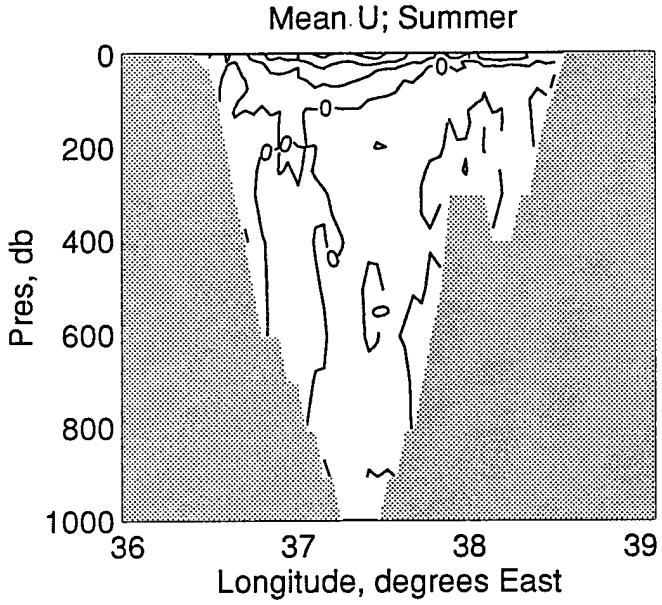

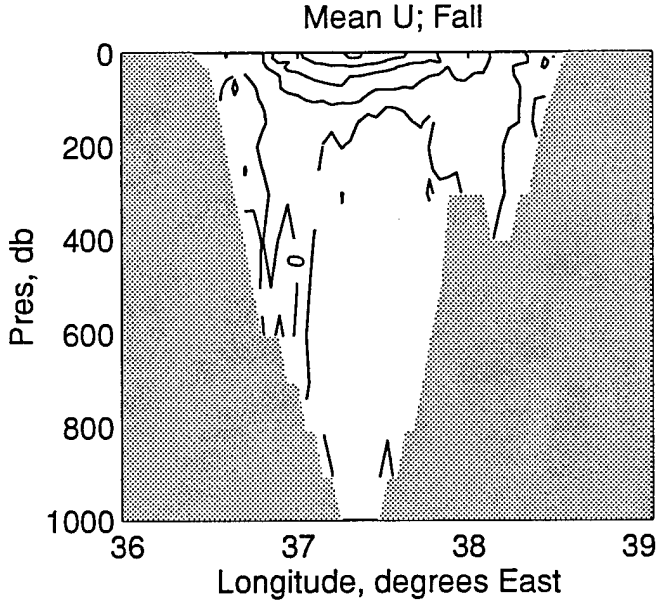

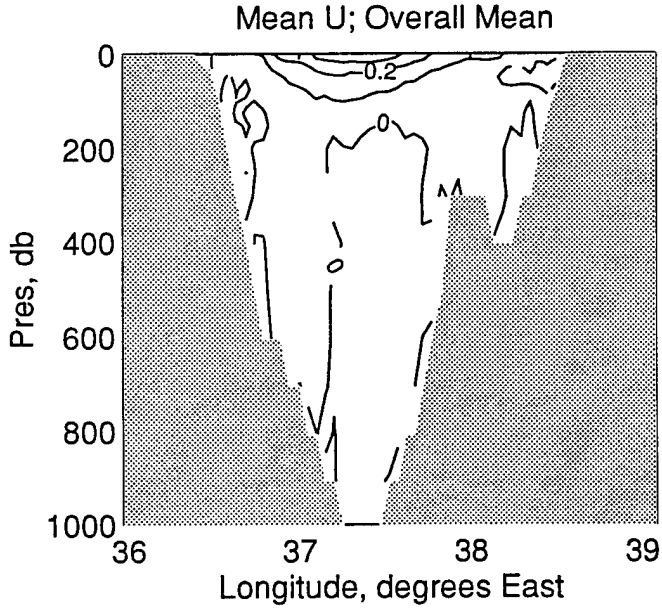

RED SEA MODEL DATA

Central Lattitude = 22.9 Degrees North

Figure A7

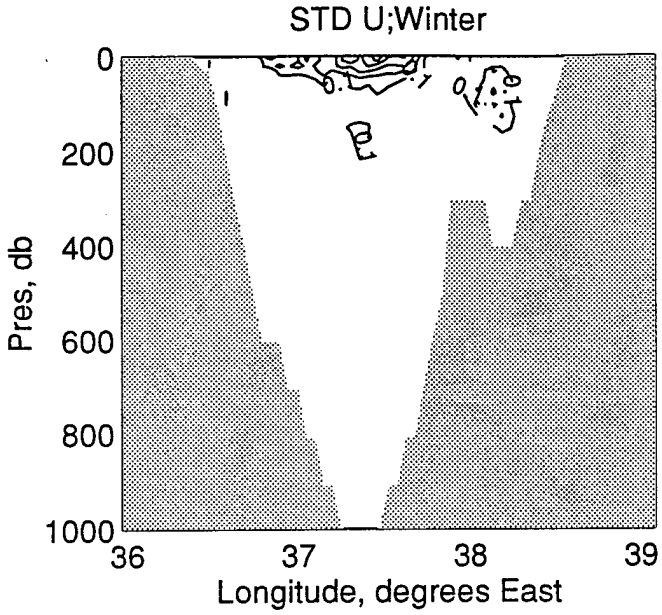

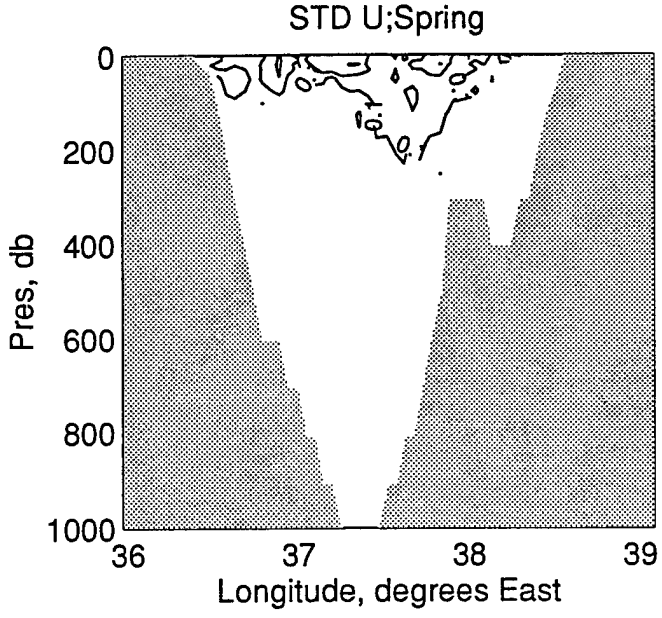

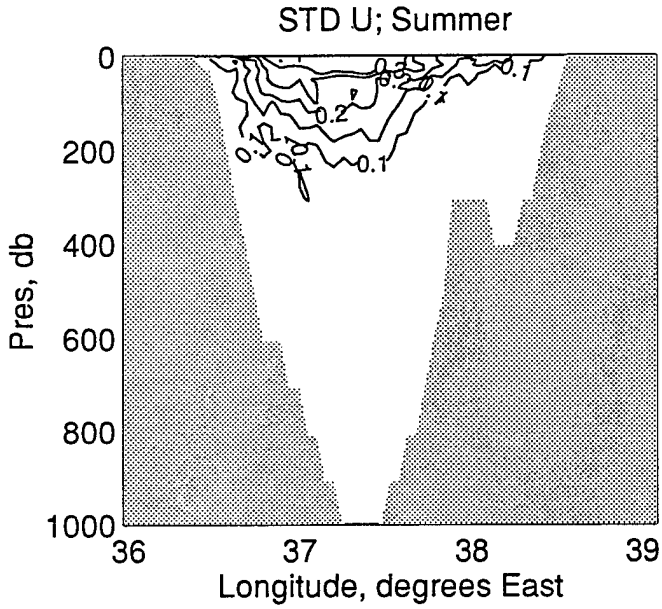

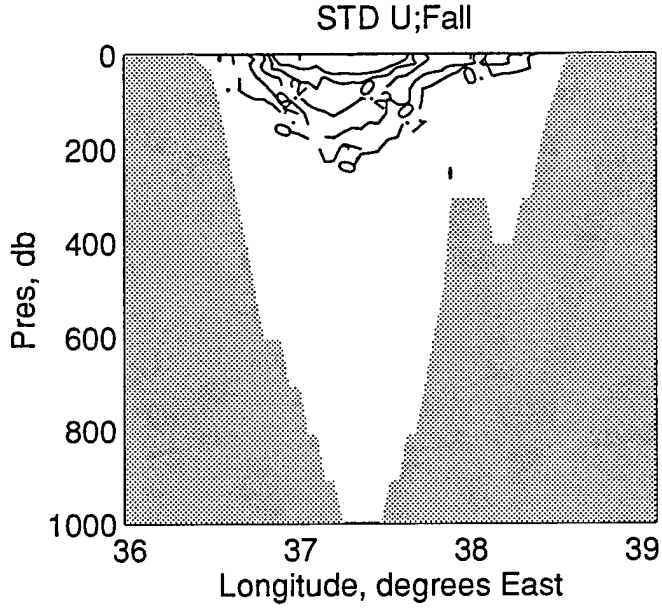

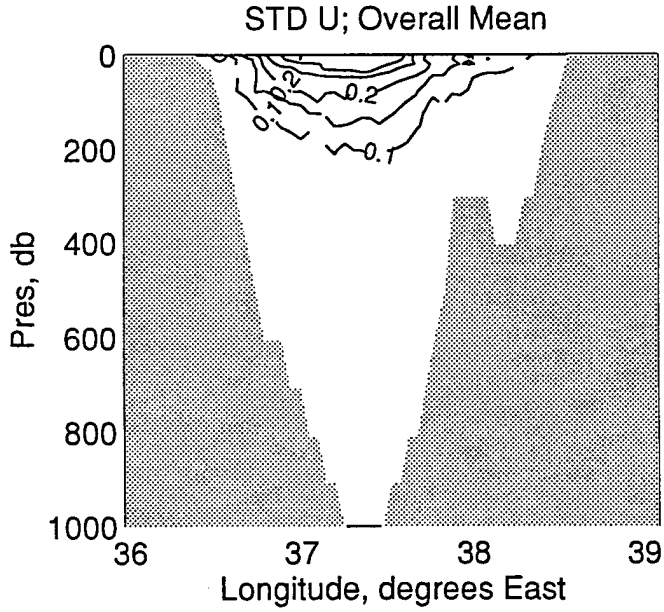

RED SEA MODEL DATA

Central Lattitude = 22.9 Degrees North

Figure A8

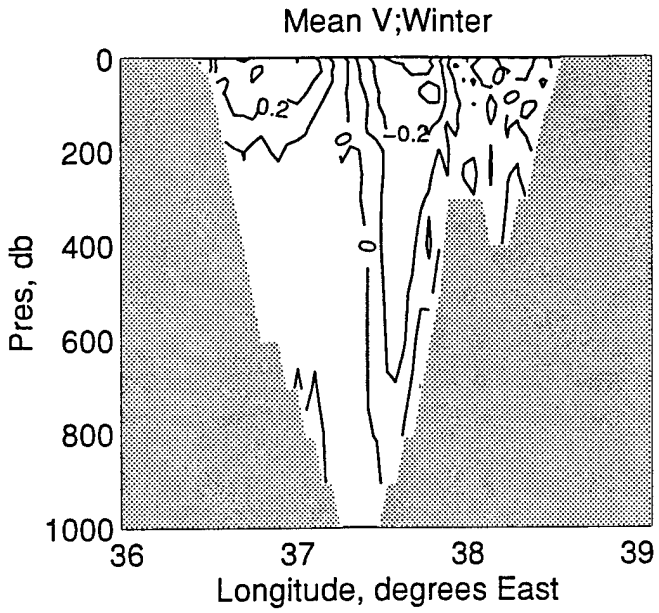

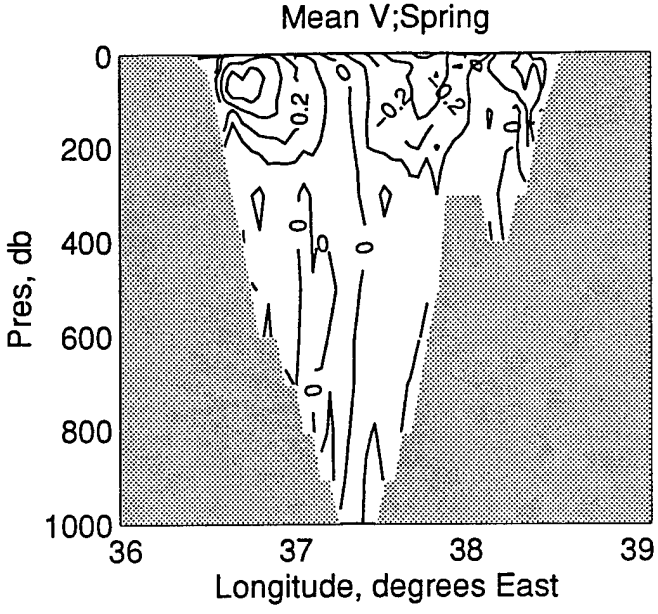

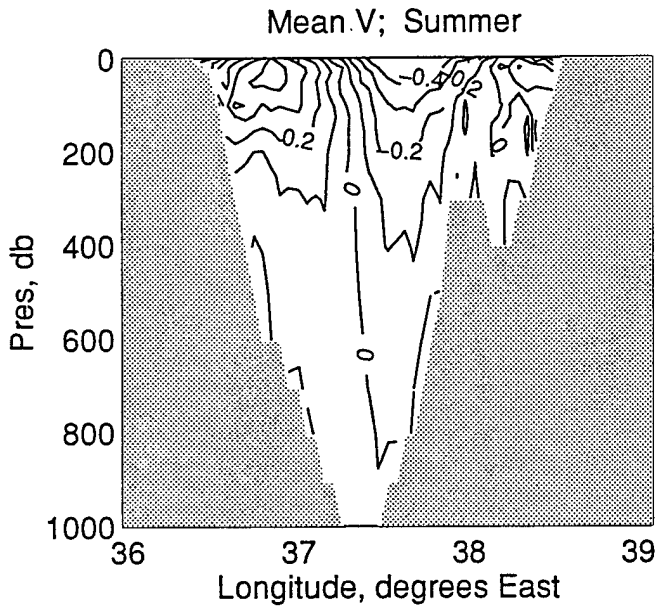

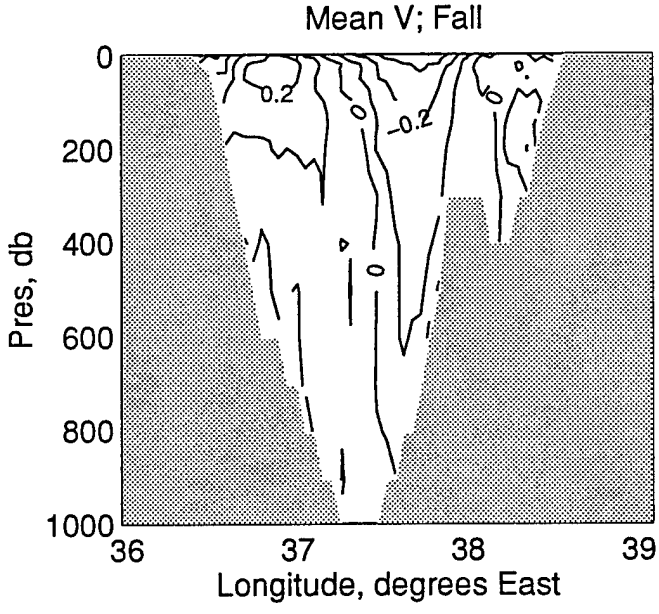

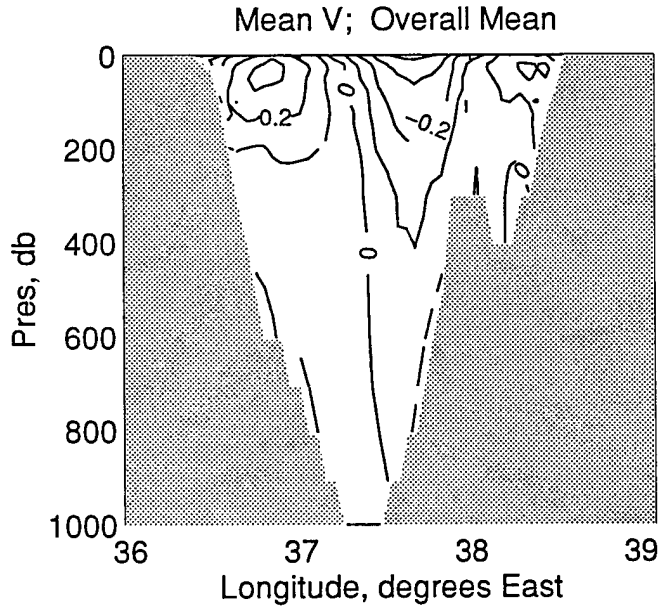

RED SEA MODEL DATA

Central Lattitude = 22.9 Degrees North

Figure A9

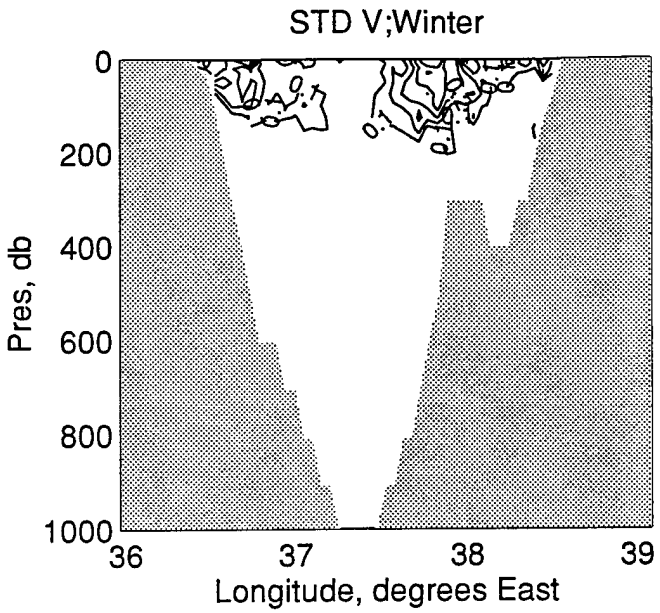

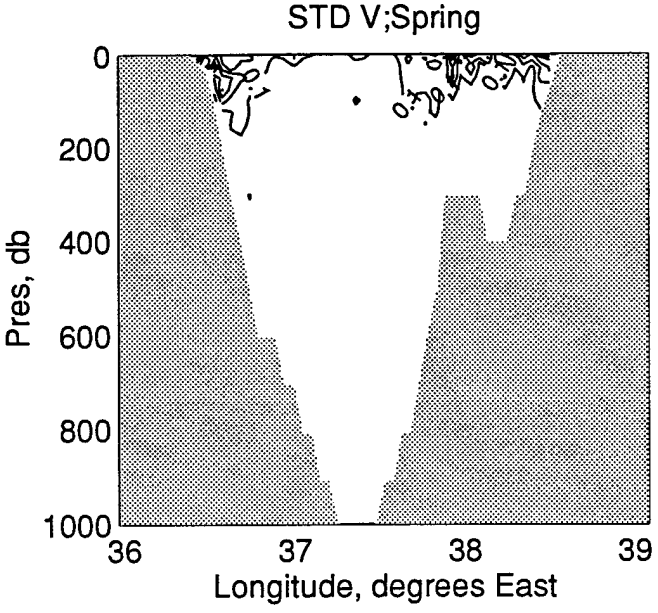

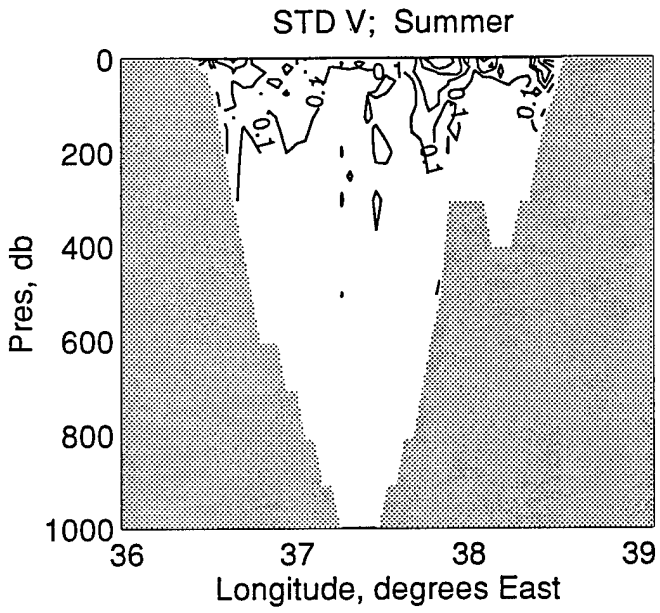

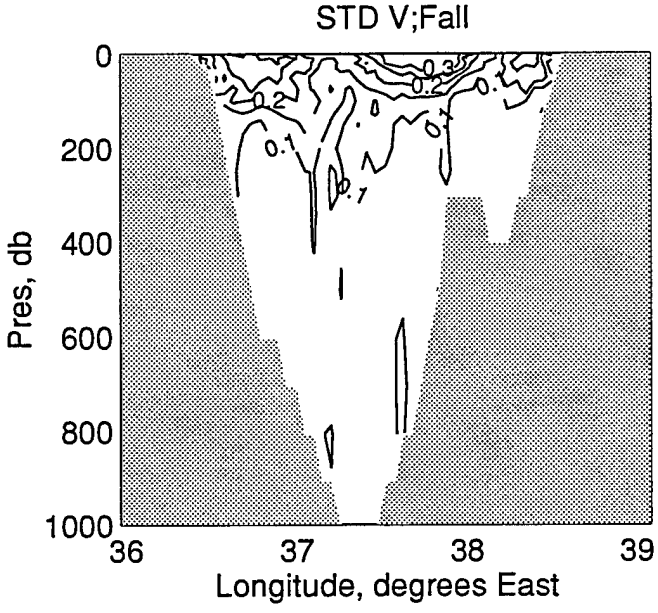

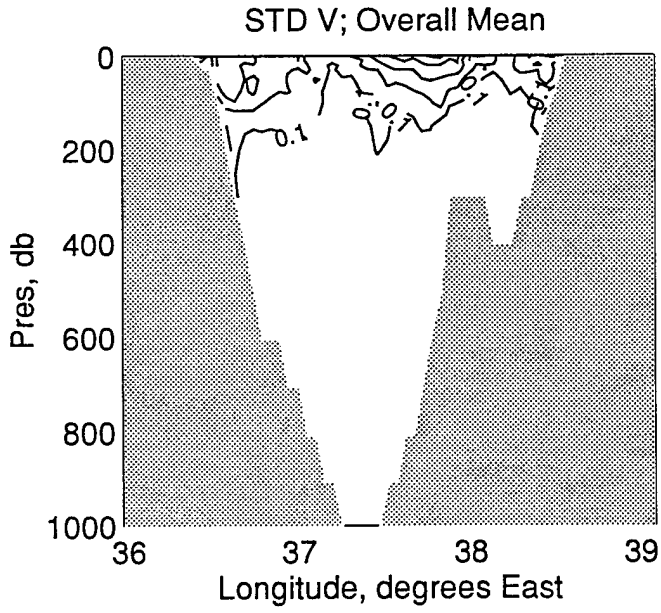

RED SEA MODEL DATA

Central Lattitude = 22.9 Degrees North

Figure A10.